processes

MDPI

Article

Effects of Biochar Addition on Gaseous Emissions During the Thermophilic Composting Phase and Subsequent Changes in Compost Characteristics

Ibrahim A. Abdelfadeel [1,*], Khaled D. Alotaibi [1,*], Fahad N. Alkoiak [2], Saud S. Aloud [1] and Ronnel B. Fulleros [2]

[1] Soil Science Department, College of Food and Agriculture Sciences, King Saud University, Riyadh 13362, Saudi Arabia
[2] Agricultural Engineering Department, College of Food and Agriculture Sciences, King Saud University, Riyadh 13362, Saudi Arabia
* Correspondence: 442106997@student.ksu.edu.sa or i.ahmed264@gmail.com (I.A.A.); khalotaibi@ksu.edu.sa (K.D.A.)

Abstract

The composting of organic waste is a sustainable strategy for waste management and soil fertility improvement. However, the composting process is often associated with greenhouse gas (GHG) emissions, having a negative impact on the environment. This study investigated the effects of BC pyrolysis temperature (300 °C, 600 °C) and application rate (5% and 10%) on GHG emissions during the thermophilic phase and compost quality. The experimental treatments were a control and four BC treatments varying in pyrolysis temperature (300 °C, 600 °C) and application rate (5%, 10%). As a result, BC pyrolyzed at 600 °C and added at 10% (T2R2) resulted in the highest thermophilic temperature (63.5 ± 0.5 °C). This treatment significantly achieved substantial reductions in NH_3, N_2O, CH_4, and CO_2 emissions by 55 ± 2.7%, 50 ± 2.7%, 88 ± 4.2%, and 23 ± 2.3%, respectively, relative to the control. Compost quality was enhanced notably, with dry matter increasing to 46.4 ± 0.11% (T2R1), organic matter reaching 30.9 ± 0.05% in T2R1, and total nitrogen peaking at 0.8 ± 0.001% (T1R2). The C:N ratio decreased from 27:1 in the control to 21:1 in the treatment of T1R2, indicating an accelerated composting process. The NH_4-N levels were the highest in T1R2 and T2R2 (659 ± 0.1 and 416 ± 0.2 mg kg^{-1}), while EC increased to 9.5 ± 0.006 ms/cm (T2R1), and bulk density decreased to 410 ± 0.08 kg/m^3 (T1R1). These results demonstrate that high-temperature biochar, especially at a rate of 10%, is effective in reducing emissions and improving compost quality. Future research should explore long-term effects and microbial mechanisms to optimize biochar use in composting systems.

Keywords: date palm waste composting; pyrolysis; biochar amendment; greenhouse gas mitigation; ammonia emissions; compost quality

Received: 16 September 2025
Revised: 3 October 2025
Accepted: 5 October 2025
Published: 9 October 2025

Citation: Abdelfadeel, I.A.; Alotaibi, K.D.; Alkoiak, F.N.; Aloud, S.S.; Fulleros, R.B. Effects of Biochar Addition on Gaseous Emissions During the Thermophilic Composting Phase and Subsequent Changes in Compost Characteristics. *Processes* **2025**, *13*, 3210. https://doi.org/10.3390/pr13103210

1. Introduction

Composting is a valuable process for transforming organic waste into a stable product, named compost, that can be used as an amendment to improve soil properties and to provide nutrients for plants [1]. However, the composting process can result in greenhouse gas emissions (GHGs), such as methane (CH_4) and nitrous oxide (N_2O), and carbon dioxide (CO_2) in addition to ammonia (NH_3) into the atmosphere [2], and this can contribute to air

pollution and environmental degradation [3]. Therefore, it is always a priority to find an effective method to reduce GHG and NH_3 emissions in the composting process and also to improve the resulting compost quality. This can include using effective additives in the composting process, such as biochar.

Biochar (BC), a stable carbon-rich material produced through the pyrolysis of biomass under oxygen-limited conditions, has emerged as a promising tool for carbon sequestration and GHG mitigation [4]. Its unique physical and chemical properties, including high porosity, surface area, and functional groups, offer potential benefits for various agricultural and environmental applications [5]. The benefits of BC application to agricultural soils have widely been documented, including the improvement of soil fertility and water retention as well as promoting crop growth and production [6–9]. Moreover, BC has recently been proposed as an effective additive that can reduce gaseous emissions during the composting process and enhance compost properties resulting in a better-quality compost [1,10–12]. However, this option of BC uses has not widely been explored.

Biochar has the ability to modify nutrient cycling and redox conditions, and this could influence the production and consumption of GHGs within the composting environment [13]. However, the effectiveness of BC in mitigating GHG emissions from composting is dependent on several factors, including biochar production conditions, application rate, and the characteristics of the composting feedstock [14]. BC is gaining recognition as a valuable additive to composting systems, playing a key role in reducing GHG emissions [15]. Its porous structure and surface properties help trap volatile compounds like ammonia; it prevents it from being transformed by microbes into nitrous oxide, a harmful greenhouse gas [10,12]. Recent findings from Ref. [16] confirmed that using BC with a 10% rate in recycled manure solids (RMS) resulted in reduced cumulative CO_2 and N_2O emissions and decreased the global warming potential by 32% compared to untreated RMS. However, the 2.5% rate raised CO_2 emissions probably due to the stimulation of microbial activity. Moreover, Ref. [17] demonstrated that BC produced at 650 °C and added at a 3–6% rate could mitigate CO_2 emissions during composting by 80%. A meta-analysis study which reviewed 105 papers with 414 observations from 15 countries suggests that BC can significantly lower N_2O and CH_4 emissions by shaping microbial activity and promoting a more oxygen-rich environment within compost piles [11]. Fine-tuning BC attributes—such as the choice of feedstock, pyrolysis conditions, and application methods—can enhance its ability to minimize the GHG impact of composting.

For biochar to be widely adopted economically, it is essential to comprehend the feasibility of employing it at various application rates and pyrolysis temperature. While increased application rates may result in improved compost quality and emission management, yet increase input costs, producing BC at higher pyrolysis temperature may enhance its stability and benefits but also raise energy costs. Therefore, the priority is in identifying its practical use in composting systems which requires finding the most cost-effective integration of pyrolysis temperature and BC dosage that offers the most agronomic and environmental advantages without imposing excessive expenditures.

Saudi Arabia's substantial date palm cultivation generates a significant volume of organic residues, including leaves, fronds, and date pits. These residues are valuable feedstocks for producing BC, which has a potential use as an additive for enhancing compost quality and mitigating GHG emissions. However, while BC has been widely studied in general composting contexts, there is still limited understanding of how the pyrolysis temperature which strongly influences BC's surface area, porosity, pH, and functional groups and the application rate which determines the extent of interaction with composting substrates, specifically affect GHG and NH_3 emissions during the composting process... Previous studies often investigated the single application rate or fixed pyrolysis

temperature, leaving uncertainty about the magnitude and direction of effects when these two critical factors vary simultaneously. This knowledge gap restricts the ability to optimize BC use for maximum environmental benefits. Therefore, this study aimed to investigate how the pyrolysis temperature and addition rate affect the role of using BC as a composting additive, particularly focusing on its impact on GHG and NH_3 emissions and changes in compost characteristics during the thermophilic stage. The findings will provide new insights into tailoring BC properties and application strategies, thereby contributing to more environmentally friendly composting practices and promoting the use of BC in agricultural and environmental applications.

2. Material and Methods

2.1. Biochar Production

Date palm residues (DPR), the feedstock used to produce BC, were collected from a private farm near Riyadh city, air-dried and crushed into small pieces. The DPR was then placed in a stainless chamber, tightly sealed to ensure oxygen-limited conditions and placed into a Digital Muffle Furnace (Model FH-12, DAHAN Scientific Co., Ltd., Gangwon-do, Republic of Korea). The initial biomass of DP (trunk) was air-dried, chopped to 5 cm-long pieces and then grinded to a particle size of approximately 5 mm before pyrolysis. Thereafter, it was pyrolyzed at two temperatures: 300 °C and 600 °C, referred to as T1 and T2, respectively. These temperatures were chosen to represent low and high pyrolysis regimes, which are known to produce BC with distinct properties. Low temperature BC (300) °C typically retains more volatile matter and functional groups, enhancing microbial activity and nutrient retention. Meanwhile, BC produced at higher temperature (600) °C is more carbon-rich, porous, and stable, offering better performance for GHG emission and long-term carbon sequestration. The selection of these temperatures was guided by previous studies (e.g., [10,18,19]) to explore how BC properties influence composting outcomes. After pyrolysis, the BC was cooled, and ground, and sieved to a uniform particle size of 2 mm.

Basic Characteristics of Biochar Products:

Table 1 presents the basic characteristics of BC derived from DPR pyrolyzed at two different temperatures as presented in the table below.

Table 1. Basic characteristics of date palm-derived biochar.

Variables	Pyrolysis T (300) °C	Pyrolysis T (600) °C
pH	6.84	8.75
EC (ds m^{-1})	7.27	7.86
Total C (%)	55.31	67.54
Total N (%)	0.49	0.39
Total P (%)	0.07	0.09
BET surface area (m^2 g^{-1})	3.72	162.94

Increasing the pyrolysis temperature from 300 °C to 600 °C markedly changed the properties of DP-BC. The pH and EC increased, suggesting a higher mineral concentration, while total C increased and N decreased slightly as a result of volatilization. P content revealed a slight rise. The most significant change was in surface area, rising from 3.72 to 162.94 m^2 g^{-1}, indicating improved porosity. These changes indicate that high-temperature biochar offers improved stability, adsorption capacity, and nutrient retention ability, enhancing its effectiveness as a compost additive.

2.2. Compost Feedstock Preparation

The DPR (leaves) were collected from the same source and ground into small particles up to 1–2 cm using a FYS-76-shredder (Mainland, Yongkang, China). Grinding DPR into small pieces was necessary to facilitate uniform mixing and create better aeration during the decomposition process. Compost mixtures were prepared by combining DPR and chicken manure (CM), and the BC was added to the mixture at two rates: 5% and 10%, referred to hereafter as R1 and R2, respectively. A compost mixture that received no BC was used as a control treatment (T0) for comparison. To prepare the compost, air-dried chicken manure was thoroughly mixed with DPR. The main purpose of adding chicken manure was to balance the carbon-to-nitrogen (C:N) ratio, as date palm residues tend to be high in carbon but low in nitrogen. Since chicken manure is rich in nitrogen, its inclusion helps create an optimal C:N ratio, essential for supporting microbial activity during decomposition. This balance promotes the efficient breakdown of organic matter, resulting in high-quality compost. The prepared compost mixtures were loaded into bioreactors to ensure controlled conditions and facilitate gas sampling.

Appropriate ratios of a compost mixture of CM, DPR, and water, with the optimal level of moisture content (MC) of 60% and a C:N of 30:1 were calculated according to Equations (1) and (2) [20].

$$\mathrm{MC}(\%) = \frac{(\mathrm{MC_c Q_c} + \mathrm{MC_r Q_r})}{(\mathrm{Q_c} + \mathrm{Q_r})} \quad (1)$$

$$(\mathrm{C:N}) = \frac{\{\mathrm{C_c Q_c}(100 - \mathrm{MC_c}) + \mathrm{C_r Q_r}(100 - \mathrm{MC_r})\}}{\{\mathrm{Q_c N_c}(100 - \mathrm{MC_c}) + \mathrm{N_r Q_r}(100 - \mathrm{MC_r})\}} \quad (2)$$

where MC, Q, C, and N are the moisture content (%), mass (kg), carbon content (%), and nitrogen content (%) of the chicken manure (subscript c), and PDR (subscript r), respectively, (Table 2).

Table 2. Some raw material properties and final quantity for composting.

Material	MC	C%	N%	C:N	Quantity (Q)	Total Mixture for Each Treatment Q/kg
Date palm residues	7.3	43.51	0.75	58:1	12 kg	-
Chicken manure	9.63	43.88	2.9	15:1	6 kg	-
Water	100	0	0	-	23.4 L	
Total (Treatment without biochar)						41.4 (Bioreactor 1)
Quantity after biochar addition						
Biochar pyrolyzed at 300 °C (5%)					0.9 kg	42.3 (Bioreactor 2)
Biochar pyrolyzed at 300 °C (10%)					1.8 kg	43.2 (Bioreactor 3)
Biochar pyrolyzed at 600 °C (5%)					0.9 kg	42.3 (Bioreactor 4)
Biochar pyrolyzed at 600 °C (10%)					1.8 kg	43.2 (Bioreactor 5)
Confirmation						
C:N ratio after mixing	28:1					
Mixture initial moisture content (%)	60					

2.3. Bioreactor Design and Treatment Application

Three identical pilot-scale bioreactors, each with a volume of 0.2 m^3, constructed in the laboratory of the Agricultural Engineering Department at the educational farm of the College of Food and Agriculture Sciences, King Saud University were used for compost

production in the current study [21]. Each bioreactor was a steel barrel with an inner diameter of 585.0 mm, a length of 914.4 mm, and a wall thickness of 3.0 mm (Figure 1A,B). Each bioreactor was designed to provide a space for 50 kg (wet bases) of compost mixture as well as 25% of the volume as a headspace.

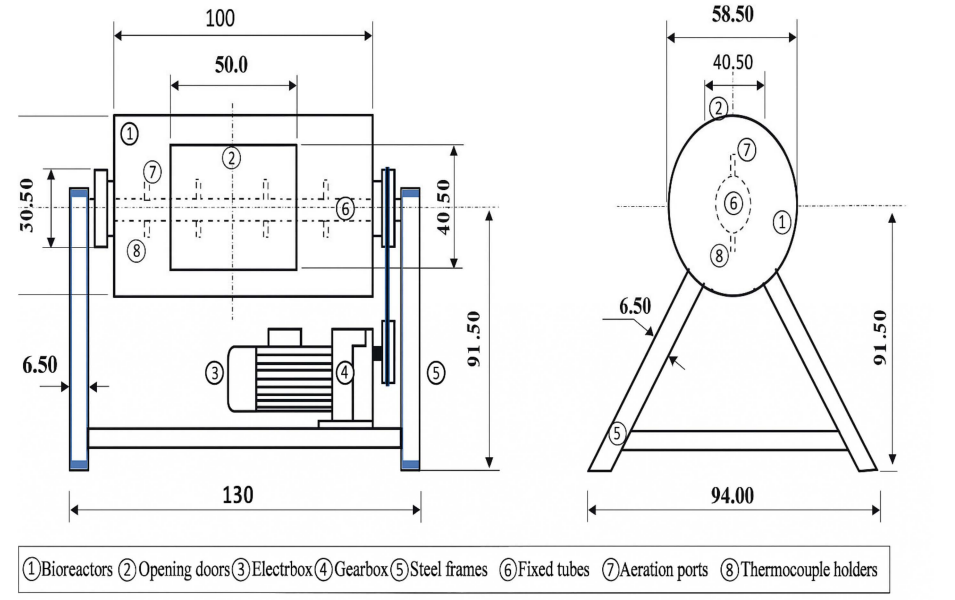

(**A**)

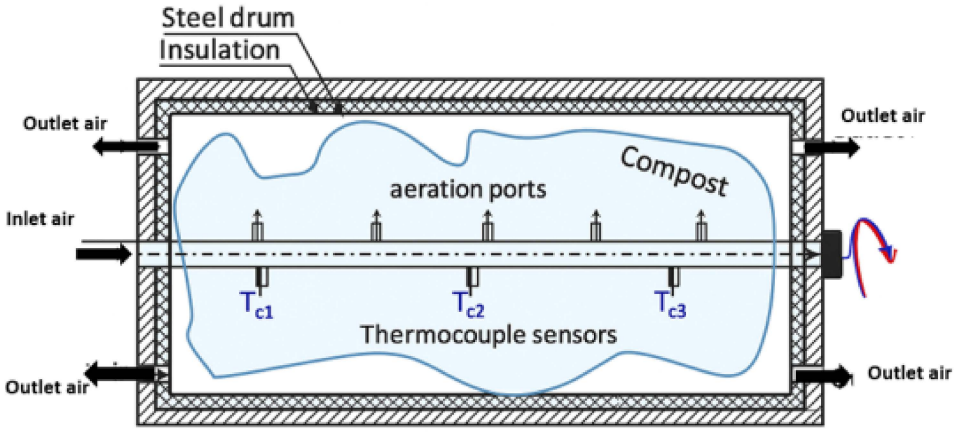

(**B**)

Figure 1. Diagram designed by [21] illustrating the design of the rotary-drum bioreactor system (**A**) (dimensions in centimeters); (**B**) cross-sectional view of the drum highlighting the positions of the aeration inlet and outlet ports, as well as the placement of thermocouple sensors.

Briefly, the outer surface of the bioreactor was insulated with glass wool to prevent heat loss and enhance metabolic exothermic reactions (25 mm thick). The bioreactor was rotated at 3 rpm around its axis (i.e., a fixed tube with a 50 mm outer diameter). For aeration purposes, the perimeter of the tube included holes distributed longitudinally along the upper surface of the tube in the rotating bioreactor. The bioreactors were running under aerobic conditions for a period of nine days to allow for the thermophilic phase of composting. Each material mixture of each compost type was placed into one bioreactor for the thermophilic stage of nine days The study consisted of five experimental treatments: (1) a control, composting without BC addition (T0); (2) biochar produced at 300 °C and added at 5% (T1R1); (3) biochar produced at 300 °C and added at 10% (T1R2); (4) biochar

produced at 600 °C and added at 5% (T2R1); (5) biochar produced at 600 °C and added at 10% (T2R1).

2.4. Measurement of Temperature

The temperatures of each compost type were measured every 30 min during the thermophilic stage by using three copper–constantan thermocouples (Tc1, Tc2, and Tc3) (type-T, Cole Parmer, Chicago, IL, USA) in each bioreactor, and Tc was estimated as the average value of Tc1, Tc2, and Tc3. The three thermocouple wires were connected to a portable data logger (Model: Testo 177-T4 V01-02, SE & Co. KGaA, Lenzkirch, Germany) [21].

2.5. Measurement of Greenhouse Gases and Ammonia Emissions

The GHGs (CO_2, CH_4, and N_2O) and NH_3 emitted during the thermophilic stage of composting were measured daily over a nine-day period using a (Gasmet DX4015; Technologies Oy, Helsinki, Finland). connected directly to a Calcmet software (V1.9) instrument (Figure 2) and (Figure 1). The Gasmet DX4015 detects gases based on their unique infrared absorption spectra and has been widely validated in diverse ecosystems such as the Finnish agroecosystems [22] and Canadian High Arctic soils [23]. Prior to each measurement, the gas collection ports on the BC lids were tightly sealed for one hour to allow headspace gas accumulation. At each sampling point, three consecutive readings were taken per reactor, and the average was used to minimize measurement error. This repeated-measure approach improves data reliability and ensures statistical robustness. Comparisons were made between the treatment groups with different biochar application rates and pyrolysis temperatures to evaluate treatment effectiveness.

Figure 2. GHG emission sample collection using a Gasmet DX4015 during the thermophilic phase; the samples were taken with replicates (three reading for each GHG type).

2.6. Compost Sampling and Analysis

At the end of the thermophilic stage, which lasted nine days, compost samples were collected from three distinct zones within each bioreactor (left, center, and right) to account for possible spatial variability. The sub-samples were thoroughly homogenized to form a

composite sample per treatment to ensure representativeness. Compost samples collected after the thermophilic phase were submitted to an external lab for a comprehensive quality analysis. The laboratory followed the procedures outlined in the Test Methods for the Examination of Composting and Compost (TMECC) [24].

The analysis included key physicochemical parameters such as organic matter (OM), pH, electrical conductivity (Ec), total carbon and nitrogen (C:N), and the carbon-to-nitrogen (C:N) ratio. Macro- and micronutrient concentrations (e.g., P, K, Ca, Mg, Na, Fe, Zn, and Cu) were assessed using acid digestion and Inductively Coupled Plasma (ICP-OES) spectroscopy, all in accordance with TMECC protocols. All chemical analyses were performed in triplicate, and results are presented as means ± standard error. This standardized approach ensures a reliable evaluation of compost quality, maturity, and suitability for agricultural applications.

2.7. Data Analysis

The interaction between time (days) and BC application rates was assessed using a two-way ANOVA to evaluate their combined effects on composting dynamics. Additionally, GHG emissions, temperature variations, and compost properties were analyzed using two-way ANOVA with an all-pairwise comparison (LSD) in Origin Pro (V. 2025). This approach helped determine the influence of biochar treatments on emissions and compost characteristics at the end of the thermophilic phase.

3. Results

3.1. Temperature

Figure 3 illustrates the temperature variations observed during the composting process across all treatments over a 9-day monitoring period. A distinct thermophilic phase was evident, with treatments steadily increasing from Day 1, reaching their peak around Day 7 and subsequently declining as the system entered the cooling stage. The control (T0) consistently recorded the lowest temperatures throughout the thermophilic stage, beginning at 25.4 ± 0.6 °C on Day 1 and peaking at 55.5 °C on Day 8. In contrast, treatments incorporating biochar exhibited significantly higher temperature profiles, with biochar pyrolyzed at 600 °C (T2) demonstrating the most pronounced effect. Among these, T2R2 (10% biochar at 600 °C) achieved the highest peak temperature of 63.5 ± 0.5 °C on Day 7, followed by T2R1 at 59.5 ± 0.5 °C. Treatments containing biochar pyrolyzed at 300 °C (T1) also showed elevated temperatures compared to the control, with T1R2 and T1R1 reaching 58.5 ± 0.5 °C and 56.5 ± 0.5 °C, respectively, on Day 7.

An analysis of temperature trends over the thermophilic stage revealed a significant increase from an initial average of 28.0 ± 1.76 °C on Day 1 to a peak of 57.9 ± 4.09 °C on Day 7, followed by a decline to 42.4 ± 3.04 °C by Day 9. When assessed by treatment type and biochar application rate, the overall mean temperature was lowest in T0 (44.5 ± 8.87 °C) and highest in T2R2 (49.9 ± 10.83 °C), closely followed by T2R1 (49.4 ± 10.91 °C). This pattern highlights the positive influence of a higher pyrolysis temperature and increased biochar application rates.

Statistical analyses using two-way ANOVA confirmed the significant effects of Time (p-value < 0.0001 and F-value of 5404.94) and Treatment (p-value < 0.0001 and F-value of 433.53) on compost temperature. Additionally, a strong interaction between Time and Treatment (p-value < 0.0001 and F-value 94.64) indicated that the impact of biochar application on temperature fluctuated dynamically throughout the composting process. Post hoc LSD tests indicated that all BC treatments had significantly higher temperatures than the control ($p < 0.05$) (Table S1).

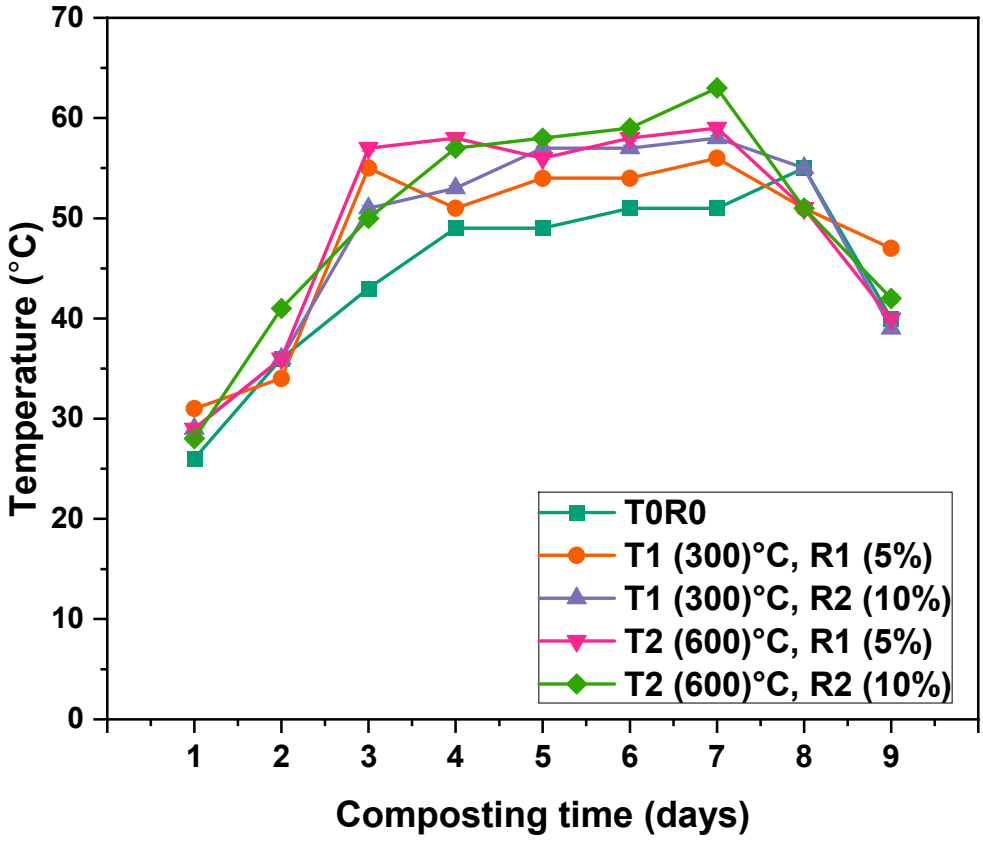

Figure 3. The temperature variation in compost bioreactors during the composting process (from Day 1 to Day 9), fluxes are mean values for three replicates, (T0) represents compost without biochar addition, while T1, T2, R1, and R2 donate biochar pyrolyzed at temperature of 300 °C and 600 °C and added at rates of 5% and 10%, respectively.

3.2. NH_3 Emissions

Figure 4 illustrates the pattern of NH_3 emissions during the composting process across various treatments. The temporal pattern of NH_3 emissions during composting exhibited distinct fluctuations across all treatments. A sharp increase was noted in the early phase (Days 3 to 6), reaching its peak on Day 6. The control treatment (T0) recorded the highest NH_3 emissions at 32.17 ± 0.12 mg kg^{-1}. In contrast, biochar-amended treatments—significantly suppressed NH3 emissions: T1R1 (17.10 ± 0.26) mg kg^{-1}, T1R2 (12.03 ± 0.3) mg kg^{-1}, T2R1 (2.2 ± 0.05) mg kg^{-1}, and T2R2 (1.82 ± 0.01) mg kg^{-1} on the same day. Following this peak, emissions declined substantially across all treatments. By Day 9, NH_3 emissions had dropped to 10.4 ± 0.12 (T0), 1.23 ± 0.009 (T1R1), 0.78 ± 0.005 (T1R2), 0.21 ± 0.003 (T2R1), and 0.3 ± 0.008 (T2R2). The reduction was more substantial in BC-amended composts, especially those with higher application rates. The cumulative mean NH_3 emissions over the composting period followed a decreasing order: T0 > T1R1 > T1R2 > T2R1 > T2R2, with mean values of (18.19 ± 1.3, 8.63 ± 0.9, 7.13 ± 0.8, 5.44 ± 0.61, and 4.95 ± 0.58) mg kg^{-1}, respectively. The reduction percentages of NH_3-N showed that T2R2 achieved the highest reduction at (55 ± 2.7)%, followed by T2R1 (45 ± 3)%, T1R2 (40 ± 3.1)%, and T1R1 (30 ± 2.7)%. Statistical analysis using two-way ANOVA revealed that significant effects of time (days) ($p < 0.0001$ and F 22.44) and treatment (p-value of <0.0001, and F-value of 105.76), and their interaction ($p < 0.0001$ with an F-value of 7.47) (Table S2), this confirmed that all BC treatments were significantly different from the control.

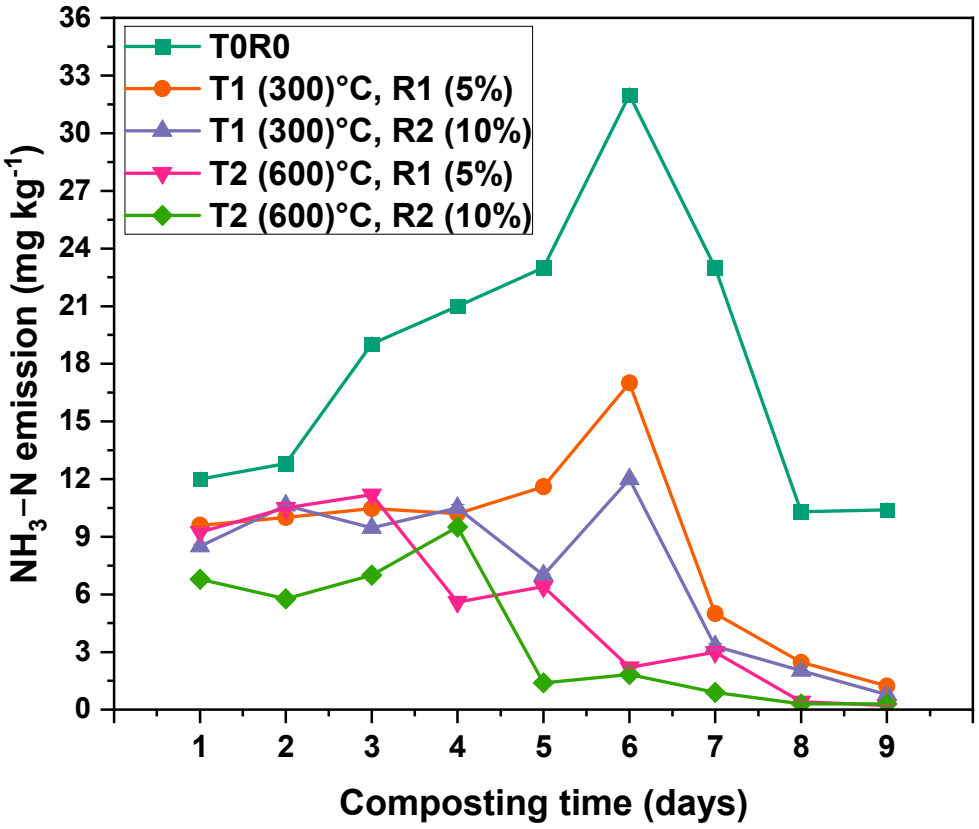

Figure 4. NH_3-N loss rate during the composting process from Day 1 to Day 9 of the thermophilic phase. Fluxes are the mean values ± standard error (SE) of three replicates (n = 3). T0—date palm compost without biochar, T1R1—date palm compost amended with biochar pyrolyzed at 300 °C and added at 5% rate during composting, T1R2—date palm compost amended with biochar pyrolyzed at 300 °C and added at 10% rate during composting, T2R1—date palm compost amended with biochar pyrolyzed at 600 °C and added at a 5% rate during composting, T2R2—date palm compost amended with biochar pyrolyzed at 600 °C and added at a 10% rate during composting. At the 0.05 level, the interaction between time (days) and BC rate is significant ($p < 0.001$).

3.3. N_2O Emissions

Figure 5 illustrates nitrous oxide (N_2O) emissions during the composting process. The highest peak emissions were recorded in the early stages, particularly between days 2 and 5. Peak emissions occurred on Day 2, with 9.47 ± 0.008 mg kg^{-1} recorded in T0, followed by 6.4 ± 0.003 mg kg^{-1} in T1R1. Conversely, treatments incorporating BC, especially T1R2, T2R1, and T2R2 showed significantly lower N_2O emissions throughout the thermophilic phase. Among these, T2R2 displayed the lowest overall values, ranging from 0.02 ± 0.0017 to 0.48 ± 0.009 mg kg^{-1}, while T2R1 and T1R2 exhibited ranges of 0.03 ± 0.005 to 0.65 ± 0.006 mg kg^{-1} and 0.04 ± 0.006 to 1.88 ± 0.01 mg kg^{-1}, respectively. By Day 5, emissions in T0 dropped to 3.39 ± 0.009 mg kg^{-1}, whereas T2R2 maintained emissions as low as 0.35 ± 0.009 mg kg^{-1}. From Day 6 onward, all treatments exhibited relatively stable and reduced emissions. Compared to the control, cumulative reductions in N_2O emissions were measured as follows: T2R2 (50 ± 2.4)%, T2R1 (43.1 ± 2.1)%, T1R2 (36.2 ± 1.3)%, and T1R1 (29.2 ± 1.9)%. Two-way ANOVA confirmed significant effects of time (p-value < 0.001 and F-value 14,443.68), and treatment (p-value < 0.001 and F-value 40,761.01), and their interaction (p-value < 0.001 with F-value of 3143.91) (Table S3).

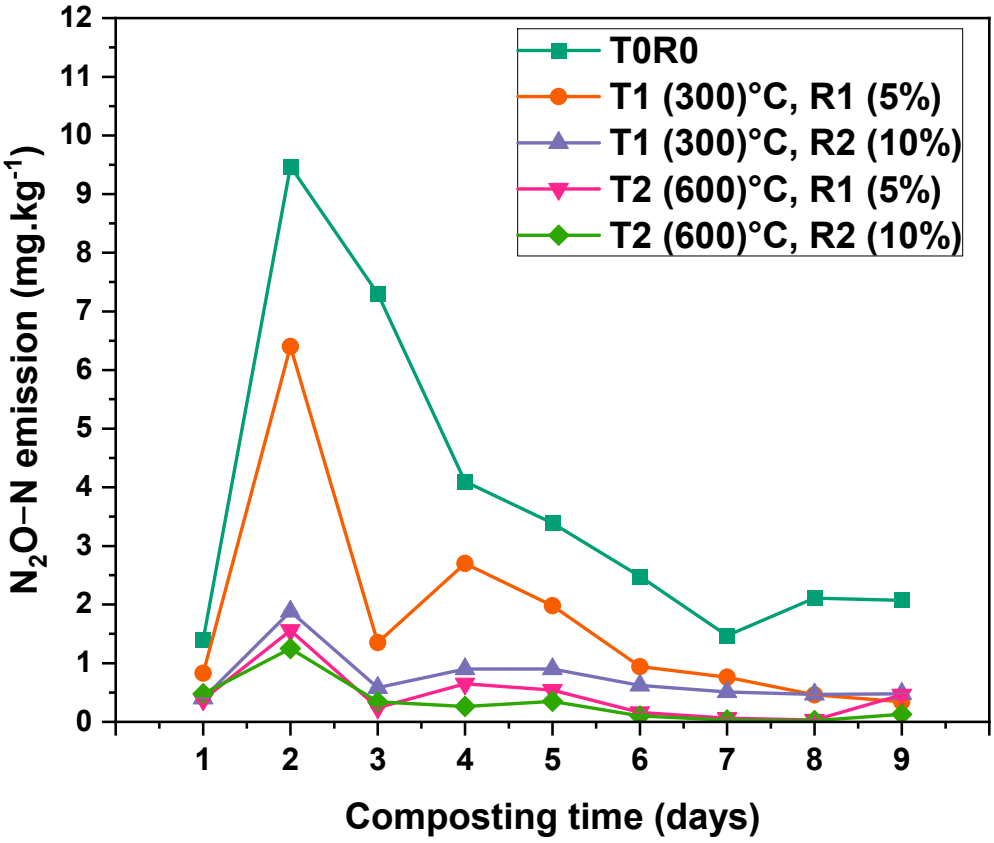

Figure 5. N_2O-N emission rate dynamics during the composting process from Day 1 to Day 9 of the thermophilic phase. Fluxes are mean values ± standard error (SE) of three replicates (n = 3). T0—date palm compost without biochar, T1R1—date palm compost amended with biochar pyrolyzed at 300 °C and added at 5% rate during composting, T1R2—date palm compost amended with biochar pyrolyzed at 300 °C and added at 10% rate during composting, T2R1—date palm compost amended with biochar pyrolyzed at 600 °C and added at 5% rate during composting, T2R2—date palm compost amended with biochar pyrolyzed at 600 °C and added at 10% rate during composting. At the 0.05 level, the interaction between time (days) and BC rate is significant ($p < 0.001$).

3.4. CH_4 Emissions

Figure 6 presents CH_4 emissions throughout the composting period across all treatments. During the first four days, composts amended with biochar (T1R1, T1-R2, T2R1, and T2R2) exhibited relatively low CH_4 emissions. In contrast, the control treatment (T0) showed a gradual increase from Day 1 (0.012 ± 0.0001) g·kg^{-1}, reaching its highest recorded value of (0.058 ± 0.0003) g·kg^{-1} on Day 6. On Day 5, CH_4 emissions in T0 recorded (0.014 ± 0.0002) g·kg^{-1}, while peak emissions in biochar-treated composts occurred in T1R1 (0.038 ± 0.0001) g·kg^{-1}, T1R2 (0.028 ± 0.00006) g·kg^{-1}, and T2R1 (0.033 ± 0.00008) g·kg^{-1}. These treatments peaked between Days 4 and 6, followed by a decline from Day 7 onward. Meanwhile, T2R2 (biochar at 600 °C, 10%) exhibited a delayed peak, rising sharply to (0.04 ± 0.0002) g·kg^{-1} on Day 6 before decreasing to (0.021 ± 0.000005) g·kg^{-1} and (0.016 ± 0.00003) g·kg^{-1} on Days 7 and 8, respectively. By Day 9, all treatments showed a noticeable reduction in CH_4 emissions. T0 maintained a level of (0.011 ± 0.00002) g·kg^{-1}, while biochar-amended treatments recorded lower values, particularly T2R2 (0.007 ± 0.00006) g·kg^{-1} and T2R1 (0.004 ± 0.00006) g·kg^{-1}. The substantial reduction percentages were as follows: T2R2, with an (88.2 ± 4.2)%, (76.5 ± 2.2)% in T2R1, (58.8 ± 3.1)% in T1R2, and (44.1 ± 3)% in T1R1 compared to control (T0).

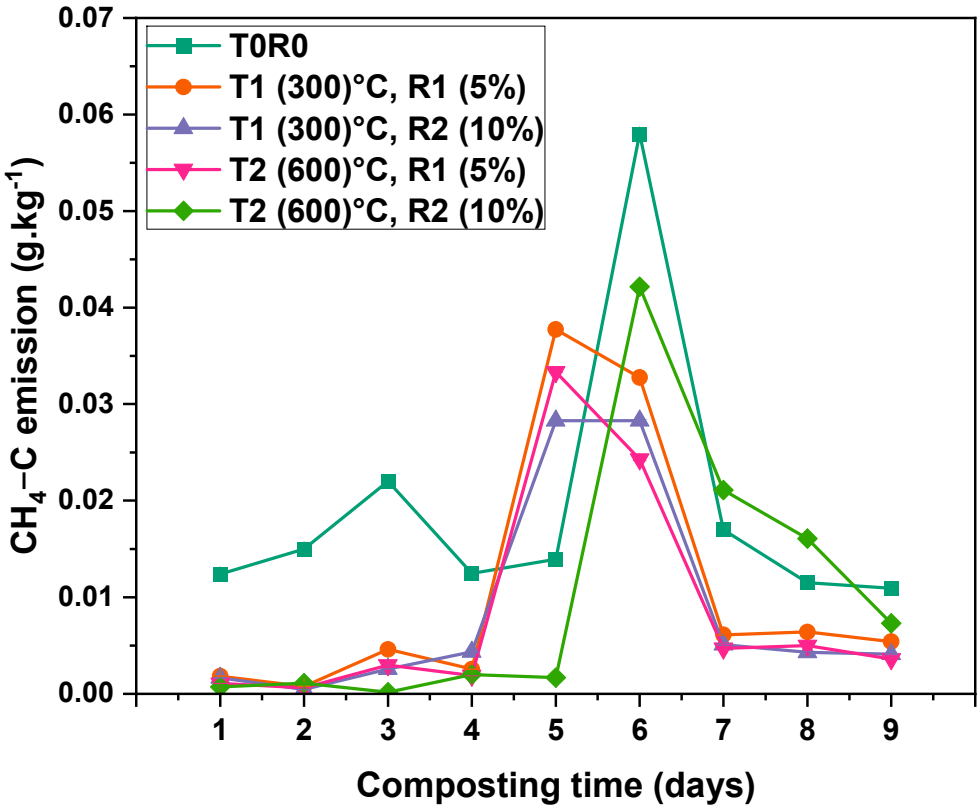

Figure 6. CH_4-C emission rate dynamics during the composting process from Day 1 to Day 9 of the thermophilic phase. Fluxes are mean values ± standard error (SE) of three replicates (n = 3). T0—date palm compost without biochar, T1R1—date palm compost amended with biochar pyrolyzed at 300 °C and added at a 5% rate during composting, T1R2—date palm compost amended with biochar pyrolyzed at 300 °C and added at a 10% rate during composting, T2R1—date palm compost amended with biochar pyrolyzed at 600 °C and added at a 5% rate during composting, T2R2—date palm compost amended with biochar pyrolyzed at 600 °C and added at a 10% rate during composting. At 0.05 level, the interaction between time (days) and BC rate is significant ($p < 0.001$).

Two-way ANOVA confirmed significant effects of time (p-value < 0.001 and F-value 57,512.77), and treatment (p-value < 0.001 and F-value 15,589.05), and the interaction between time and treatment (p-value < 0.001 and F-value 5486.47) (Table S4). This indicates that biochar's effectiveness in reducing CH_4 emissions varies depending on the composting stage.

3.5. CO_2 Emissions

Carbon dioxide (CO_2) emissions during composting are presented in Figure 7. During the first five days, emissions remained relatively low with minor fluctuations. However, the treatment containing biochar (T2R2) exhibited a noticeable increase in CO_2 emissions from the beginning, recording 3.11 g·kg^{-1} on Day 1. From Day 4 onward, a general upward trend in CO_2 emissions was observed across all treatments. CO_2 emissions peaked on Day 7, with T2R2 recording the highest value at (31.9 ± 0.00003) g·kg^{-1}, followed by T1R2 (23.91 ± 0.00003) g·kg^{-1}, and the control treatment T0 (18.94 ± 0.00003) g·kg^{-1}. In contrast, T1R1 and T2R1 exhibited the lowest emissions at this peak stage, with values of (16.08 ± 0.00003) g·kg^{-1} and (17.03 ± 0.00003) g·kg^{-1}, respectively. After Day 7, CO_2 emissions gradually declined across all treatments. By Day 9, emissions had decreased to (19.04 ± 0.00004) g·kg^{-1} (T0), (11.44 ± 0.00004) g·kg^{-1} (T1R1), (16.10 ± 0.00004) g·kg^{-1} (T1R2), (12.12 ± 0.00004) g·kg^{-1} (T2R1), and (13.03 ± 0.00004) g·kg^{-1} (T2R2). Percentage reductions: (23 ± 2.3)% for T2R2, (18.4 ± 1.5)% for T2R1, (13.8 ± 0.9)% for T1R2, and

(9.2 ± 0.7)% for T1R1. Two-way ANOVA confirmed significant effects of time (p-value < 0.001 and F-value 3.43 × 10^{10}), and treatment (p-value < 0.001 and F-value 1.16 × 10^{10}); the interaction was also highly significant (p-value < 0.001 and F-value 1.08 × 10^{9}) (Table S5).

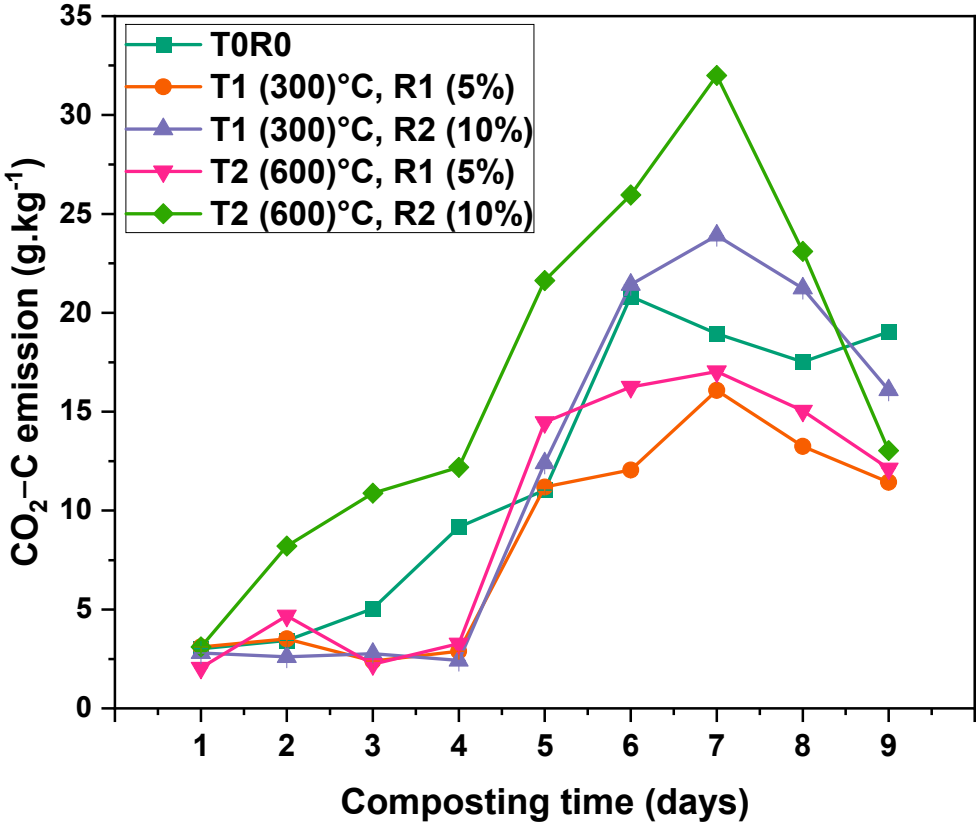

Figure 7. CO_2-C emission rate dynamics during the composting process from Day 1 to Day 9 of the thermophilic phase. Fluxes are mean values ± standard error (SE) of three replicates (n = 3). T0—date palm compost without biochar, T1R1—date palm compost amended with biochar pyrolyzed at 300 °C and added at a 5% rate during composting, T1R2—date palm compost amended with biochar pyrolyzed at 300 °C and added at a 10% rate during composting, T2R1—date palm compost amended with biochar pyrolyzed at 600 °C and added at a 5% rate during composting, T2R2—date palm compost amended with biochar pyrolyzed at 600 °C and added at a 10% rate during composting. At the 0.05 level, the interaction between time (days) and BC rate is significant (p < 0.001).

3.6. Physiochemical Properties of Compost After Thermophilic Stage

Results presented in Table 3 are the physiochemical properties after the thermophilic stage. The samples were taken at the end of the nine days of composting and sent to external laboratories for quality analysis. Consequently, after nine days of thermophilic composting, dry matter (DM) content ranged from (37.5± 0.5)% in T2R2 to (46.4 ± 0.11)% in T2R1. Organic matter (OM) showed varied percentages ranging from (26.3 ± 0.1)% in the control (T0) to (30.9 ± 0.05)% in T2R1.

The C:N ratio decreased in BC, treatments ranging from (21:1 ± 0.005) in T1R2 to (27:1) in the control. Total nitrogen (TN)% was increased in BC treatments with the highest value in T1R2 (0.8 ± 0.001)% and the lowest (0.5 ± 0.01)% in the control. Ammonium (NH_4-N) showed higher levels in treatments amended with the higher rate of biochar (10%) compared to those of (5)%. The highest level of NH_4-N appeared in (T1R2 and T2R2) with (659 ± 0.1 and 416 ± 0.2) mg kg^{-1} respectively. However, (T1R1) showed the lowest percentage (99 ± 0.06) mg kg^{-1} compared to control (399 ± 0.5) mg kg^{-1}. Meanwhile, NO_3-N showed fluctuating values ranging from 4.5 ± 0.02 mg kg^{-1} in (T2R1) to

6.2 ± 0.08 mg kg^{-1} in the control. Total phosphorus (P) showed no significant difference among all treatments and shared a similar value (0.2)%. Total potassium (K) had 0.8% for (T1R1 and T2R2) to 0.9% for (T0, T1R2, and T2R1).

Table 3. Physiochemical properties (Mean ± standard error) of compost as influenced by biochar after nine days of composting (different letters denote statistically significant differences between treatments at $p < 0.05$).

Parameter	T0	T1R1	T1R2	T2R1	T2R2	LSD
Dry matter (%)	38.2 ± 0.6 c	41.4 ± 0.7 b	43.3 ± 1.2 b	46.4 ± 0.11 a	37.5 ± 0.5 c	2.14
TN (%)	0.5 ± 0.01 e	0.6 ± 0.002 c	0.8 ± 0.001 a	0.7 ± 0.01 b	0.6 ± 0.002 d	0.03
NH4-N (mg kg^{-1})	399.0 ± 0.5 c	99.0 ± 0.06 e	659.0 ± 0.1 a	336.0 ± 0.3 d	416.0 ± 0.2 b	0.96
TP%	0.2 ± 0.004 b	0.2 ± 0.001 c	0.2 ± 0.002 a	0.2 ± 0.002 d	0.2 ± 0.005 e	0.003
TK%	0.9 ± 0.002 b	0.8 ± 0.003 d	0.9 ± 0.006 c	0.9 ± 0.002 a	0.8 ± 0.006 d	0.005
OM%	26.3 ± 0.1 e	28.1 ± 0.02 c	29.2 ± 0.1 b	30.9 ± 0.05 a	26.7 ± 0.02 d	0.35
pH	8.5 ± 0.008 a	8.3 ± 0.02 ab	8.0 ± 0.008 b	8.1 ± 0.2 a	8.2 ± 0.002 ab	0.34
EC ms/cm	6.8 ± 0.01 e	7.8 ± 0.005 d	8.9 ± 0.002 b	9.5 ± 0.006 a	8.7 ± 0.008 c	0.03
C:N	27:1 ± 0.05 a	26:1 ± 0.03 b	21:1 ± 0.05 c	26:1 ± 0.02 b	26:1 ± 0.03 b	0.05
NO^3-N (mg kg^{-1})	6.2 ± 0.08 a	4.8 ± 0.02 c	4.8 ± 0.01 c	4.5 ± 0.02 d	6.0 ± 0.08 b	0.17
BD (kg m^{-3})	496.0 ± 1.7 a	410.0 ± 0.08 e	487.0 ± 0.5 b	429.0 ± 0.08 d	438.0 ± 0.2 c	2.8
S (mg kg^{-1})	1788.6 ± 0.4 e	2233.3 ± 0.3 b	2412.0 ± 0.5 a	2184.8 ± 0.3 c	2086.2 ± 1.6 d	2.4
Ca (%)	1.8 ± 0.001 c	1.9 ± 0.002 b	2.1 ± 0.004 a	1.7 ± 0.001 d	1.7 ± 0.002 e	0.004
Mg (%)	0.2 ± 0.007 c	0.3 ± 0.006 b	0.3 ± 0.002 a	0.2 ± 0.001 c	0.2 ± 0.002 c	0.011
B (mg kg^{-1})	13.5 ± 0.1 d	15.2 ± 0.05 b	16.8 ± 0.05 a	13.8 ± 0.02 c	13.5 ± 0.05 cd	0.27
Cu (mg kg^{-1})	21.1 ± 5.4 b	24.6 ± 0.11 a	19.3 ± 0.02 ab	24.1 ± 0.05 a	17.6 ± 0.05 ab	8.01
Fe (mg kg^{-1})	1118.6 ± 0.11 e	2479.4 ± 0.5 c	3137.6 ± 0.9 b	21,786.5 ± 1.3 a	2996.7 ± 1.4 b	3.1
Mn (mg kg^{-1})	76.0 ± 0.2 d	79.8 ± 0.02 c	86.7 ± 0.2 b	106.9 ± 0.02 a	69.6 ± 0.02 e	0.6
Zn (mg kg^{-1})	66.0 ± 0.1 c	65.8 ± 0.1 d	76.9 ± 0.05 a	67.8 ± 0.1 b	57.8 ± 0.05 e	0.42

pH values varied slightly, from (8 ± 0.008) in T1R2 to (8.5 ± 0.008) in the control. The electrical conductivity (EC) increased with BC addition, with the highest value shown in T2R1 (9.5 ± 0.006) ms/cm and the lowest in the control (6.8 ± 0.01) ms/cm. Bulk density (BD) decreased when BC was added, ranging from 410 ± 0.08 kg/m^3 in (T1R1) to 496 ± 1.7 kg/m^3 in the control treatment. Sulfur (S) ranged from 1788.6 ± 0.4 mg kg^{-1} in (T0) to 2412 ± 0.5 in (T1R2) mg kg^{-1}. Iron (Fe) increased substantially, from (1118 ± 0.11) mg kg^{-1} in (T0) to (21,786.5 ± 1.3) mg kg^{-1} in (T2R1). Boron (B) values ranged from 13.5 ± 0.1 mg kg^{-1} in the control to 16.8 ± 0.05 mg kg^{-1} in (T1R2). Zinc (Zn) increased at 76.9 ± 0.05 mg kg^{-1} in (T1R2), while manganese (Mn) showed the highest value in T2R1 (106.9 ± 0.02) mg kg^{-1}. Ca and Mg showed their highest values in T1R2 with (2.1 ± 0.004 and 0.3 ± 0.002) mg kg^{-1} respectively. According to two-way ANOVA and LSD as all-pairwise comparison, there was a significant difference among all treatments for all parameters ($p < 0.001$) except for pH and copper ($p > 0.001$).

4. Discussion

4.1. Temperature Across Treatments

The thermophilic phase is critical for organic matter decomposition during composting, characterized by a distinct and rapid temperature typically peaking around Day 7, followed by a gradual decline. In this study, biochar (BC) amendments significantly influenced the temperature dynamics of the composting process. The control treatment (T0) exhibited the lowest peak temperature at 55.5 °C, while biochar-treated composts achieved notably higher thermophilic peaks. The most pronounced effect was observed in T2R2 (10% BC at 600 °C), which reached 63.5 ± 0.5 °C on Day 7, aligning well with the optimal thermophilic range of 45 °C to 65 °C. Similarly, treatments with BC pyrolyzed at 300 °C (T1) also showed elevated temperatures compared to the control.

Statistical analysis confirmed significant effects of Time ($p < 0.0001$), Treatment ($p < 0.0001$), and their interaction ($p < 0.0001$), highlighting a strong influence of BC on sustaining thermophilic conditions. This improvement can be attributed to various mechanisms associated with BC characteristics—these include the BC porous structure, which improves aeration and gas exchange, facilitating aerobic microbial metabolism, which in turn generates more heat. Secondly, BC offers a favorable microhabitat for thermophilic microbes, helping sustain microbial biomass activity. Lastly, the thermal insulation properties of BC help retain heat within the compost matrix, thereby prolonging the thermophilic phase. These mechanisms collectively describe the consistent elevation in temperature in BC-amended treatments, promoting faster decomposition, effective pathogen reduction, and enhanced compost stability. While forced aeration was employed in this study to ensure adequate oxygenation, the temperature differences among treatments are primarily attributed to the BC amendments, rather than aeration alone. This aligns with the existing literature that supports BC's role in enhancing microbial activity and thermal regulation during composting, e.g., [2,25–31]. Thus, the results reinforce the potential of BC as a valuable composting additive to enhance thermophilic performance and compost quality. Furthermore, our results underscore the importance of maintaining compost temperatures within the ideal range of 45 °C to 65 °C, as highlighted by Chowdhury [28], which was consistently achieved in our biochar-amended treatments.

4.2. Effects on NH_3-N

The application of BC, at both 5% and 10% rates, accelerated the composting process, and application rates significantly reduced NH_3 emissions during the thermophilic phase. This acceleration is likely due to enhanced microbial activity and improved nitrogen retention mechanisms. BC contributes to the stabilization of NH_{4+} through both physical adsorption and cation exchange, limiting its transformation into gaseous NH_3. Furthermore, BC develops pore microhabitats favorable for the proliferation of nitrifying bacteria (e.g., Nitrosomonas. Nitrobacter) that oxidize NH_4^+ into NO_3^-, thereby reducing NH_3 volatilization. Chen [30] demonstrated that adding BC at (2%–10%) to chicken manure significantly reduced NH_3 emissions compared to the control treatment. Similarly, the authors of Ref. [31] found that 4% of the BC rate significantly increased nitrate (NO_3^-) concentration in mature compost from 137.7 to 323.7 mg kg^{-1} and reduced nitrogen loss by 3.2 kg per ton of treated waste. Agyarko-Mintah [32] observed that 10% BC decreased total nitrogen losses by 51% and NH_3 losses by 60% in poultry litter compost. Moreover, Chen [30] has also demonstrated that BC pyrolyzed at 550–600 °C and applied at 10% reduced NH_3 losses by 24.2–56.9%. These findings suggest that BC alters N transformation pathways by improving conditions for microbial nitrification and minimizing NH_3 volatilization. The surface area and pH-buffering capacity of BC also enhance microbial resilience and activity during peak thermophilic conditions.

4.3. Effects on GHGs (N_2O, CH_4, and CO_2)

The reduction in nitrous oxide (N_2O) emissions in treatments T1R2, T2R1, and T2R2 highlights biochar's significant role in mitigating nitrogen losses. This effect may be attributed to the suppression of denitrifying bacteria (Pseudomonas, Paracoccus) under improved aeration and pH conditions promoted by BC. The BC porous structure enhances oxygen diffusion, which suppresses anerobic microzones and inhibits N_2O-producing microbial pathways. This finding is supported by Wang's [33] and Reference [34]'s investigations, who reported that BC at a 10% rate resulted in reduced N_2O emissions during the composting process. Our results align with Chen [30] and Yang [35], who reported significant reductions of N_2O (19–27)% and 46.61%, respectively, compared to the control. Additionally, N_2O emissions were reduced by 56–57% in humanure and cattle manure composts due to BC addition [36]. This underscores its robust mitigation potential.

Higher methane (CH_4) emissions observed on Days 5 and 7 are likely due to enhanced microbial activity under a high thermophilic temperature. However, BC significantly reduced CH_4 emissions compared to the control. The significant differences ($p < 0.001$) in CH_4 emissions among treatments (T1R1, T1R2, and T2R1, T2R2) during the initial seven days, as confirmed by the two-way ANOVA analysis, highlight the substantial impact of BC treatment on early CH4 release. These findings align with the authors of Reference [30], who reported 9.3–55.9 reductions in CH_4 emissions with 10% BC (550–600) °C, and authors of Ref. [36] who documented remarkable reductions (91)% in cattle manure compost. Reference [37] also demonstrated that total CH_4 emissions reduced by (15.5–26.)% with a 10% application rate derived from various feedstocks. The suppression of methanogens and the enhancement of aerobic conditions by BC likely underpins this trend.

Following the thermophilic phase (after Day 7), CO_2 emissions gradually declined across all treatments, with more pronounced reduction in T1R1 and T2R1 (5% BC) suggesting accelerated stabilization. CO_2 emissions peaked on Day 7 and this can be attributed to the rapid decomposition of labile organic matter, and intense microbial respiration (Figure 4). Although higher BC rates (10) % showed slightly elevated CO_2 in early stages, overall emissions were not increased.

These findings align with Sanchez-Monedero [38], who reported a 28% increase in CO_2 evolution with a 20% of BC addition, but no significant impact with lower doses (around 5%). Waqas [39] further confirmed that BC effectively improves the compost structure and organic matter degradation reducing net GHG emissions (CO_2, N_2O, CH_4) over time. To better understand these trends, future research should focus on the metagenomic and enzymatic profiling of microbial communities, particularly the activity of ammonia-oxidizing archaea, ammonia-oxidizing bacteria, and denitrifiers under BC-amended conditions.

4.4. Effects on Compost Characteristics

The final compost quality was significantly improved due to BC application rates during the composting process. This is likely due to the fact that BC addition results in a high cation exchange capacity (CEC), surface area, and nutrient-holding capacity. This observation is consistent with a wealth of literature [40–43]. These studies highlight how BC application, even at varying rates and pyrolysis conditions, positively influences soil physicochemical properties. Specific improvements frequently cited include an increase in CEC (20.8 to 39.0 mmol c·g^{-1}), available nitrogen (N) (3.2 to 377.2 mg kg^{-1}), available phosphorus (P) (44 to 190 mg kg^{-1}), and available potassium (K) (0.6 to 8.5 mg kg^{-1}). Furthermore, Ref. [44] reported substantial increases in CEC, P, K, and sulfur (S) in composts following BC application. The multifaceted capacity of BC to improve P availability, stabilize soil aggregates, stimulate microorganisms, and augment organic matter and

nutrient content is well-documented [30,45–47]. These effects highlight the multifaceted role of BC in improving both chemical and biological compost attributes.

While this study focused on a short term (9 days) thermophilic period, the long-term implications of BC addition—including its influence on compost curing, humus formation, and nutrient availability in field applications—warrant further investigation. Future studies should assess post-application impacts on soil health, crop productivity, and GHG fluxes to evaluate the sustainability of BC-enhanced composts in agricultural systems.

5. Conclusions and Recommendations

This study confirms that biochar, particularly when produced at a high pyrolysis temperature (600 °C) and applied at a 10% rate (T2R2), significantly enhances the composting efficiency and environmental performance of the thermophilic phase. The addition of BC accelerated microbial activity, increased peak composting temperatures, and improved nutrient retention and compost stability. Daily monitoring using a Gasmet DX4015 analyzer showed that biochar significantly reduced greenhouse gas emissions, with T2R2 achieving the greatest reductions—NH_3 decreased by 53%, N_2O by 55%, CH_4 by 61%, and CO_2 by 25% compared to the untreated control.

These benefits are attributed to BC's high porosity, adsorption capacity, and its ability to modify the microbial habitat and aeration within the compost matrix. Beyond improving compost quality, the findings suggest that BC serves as a multifunctional tool in broader sustainable agriculture and waste management frameworks. Its use can enhance soil fertility, reduce nitrogen loss, and contribute to climate change mitigation efforts. In addition, BC-enriched compost can also serve as a long-term soil amendment, improving soil structure and water-holding capacity. Nonetheless, although the 10% rate at 600 °C demonstrated the best environmental performance, further research should include an economic evaluation to harmonize efficiency with cost-effectiveness, thus enhancing the practical applicability of BC in composting systems.

This study recommended that high-temperature biochar (600 °C) can be used at a possible application rate of 10% as an effective amendment in mitigating GHG and NH_3 emissions during composting processes while improving compost quality. Environmental agencies and policymakers should consider integrating biochar-amended composting into national waste management as well as climate mitigation strategies in regions where organic waste disposal and nitrogen loss are major concerns. Furthermore, the production of biochar from locally available agricultural residues should be supported to promote resource efficiency, reduce biomass burning, and stimulate rural green economies. Finally, and also importantly, future research is needed to evaluate the long-term role of adding biochar during composting in enhancing soil health, crop productivity, and carbon sequestration under field conditions. Such studies would strengthen the case for mainstreaming biochar use in composting systems and help quantify its broader environmental and agronomic benefits over time.

Supplementary Materials: The following supporting information can be downloaded at: https://www.mdpi.com/article/10.3390/pr13103210/s1, Table S1: Two-way ANOVA results of the effects of time, treatment (T) and their interaction on compost temperature during thermophilic stage; Table S2: Two-way ANOVA results of the effects of time, treatment (T) and their interaction on NH_3 emission during thermophilic stage; Table S3: Two-way ANOVA results of the effects of time, treatment (T) and their interaction on N_2O emission during thermophilic stage; Table S4: Two-way ANOVA results of the effects of time, treatment (T) and their interaction on CO_2 emission during thermophilic stage; Table S5: Two-way ANOVA results of the effects of time, treatment (T) and their interaction on CH_4 emission during thermophilic stage.

Author Contributions: Conceptualization, I.A.A., K.D.A. and F.N.A.; methodology and formal analysis, I.A.A. and K.D.A.; data curation, I.A.A., K.D.A., F.N.A. and R.B.F.; writing—original draft preparation, I.A.A. and K.D.A.; writing—review and editing, I.A.A., K.D.A., F.N.A., S.S.A. and R.B.F.; supervision, K.D.A. and F.N.A. All authors have read and agreed to the published version of the manuscript.

Funding: This research project was funded by the Ongoing Research Funding program, number (ORF-2025-633), King Saud University, Riyadh, Saudi Arabia.

Data Availability Statement: The original contributions presented in this study are included in the article/Supplementary Materials. Further inquiries can be directed to the corresponding author.

Acknowledgments: Authors are greatly acknowledged to King Saud University, Riyadh, Saudi Arabia, for funding support.

Conflicts of Interest: The authors declare no conflicts of interest.

References

1. Nguyen, M.K.; Lin, C.; Hoang, H.G.; Sanderson, P.; Dang, B.T.; Bui, X.T.; Nguyen, N.S.H.; Vo, D.-V.N.; Tran, H.T. Evaluate the role of biochar during the organic waste composting process: A critical review. *Chemosphere* **2022**, *299*, 134488. [CrossRef]
2. Rathnayake, J. Greenhouse Gas Emission During Composting of Different Mixing Combinations of Natural Resource By-Products. Ph.D. Thesis, Memorial University of Newfoundland, St. John's, NL, Canada, 2023.
3. Ussiri, D.A.; Lal, R. *Historical and Contemporary Global Methane Cycling*; Springer International Publishing: Cham, Switzerland, 2017; pp. 227–285.
4. Fahad, S.; Arif, M.; Jan, T.; Riaz, M.; Rasul, F. *Biochar; A Remedy for Climate Change*; Springer: Berlin/Heidelberg, Germany, 2020; pp. 151–171.
5. Zhang, C.; Liu, L.; Zhao, M.; Rong, H.; Xu, Y. The environmental characteristics and applications of biochar. *Environ. Sci. Pollut. Res.* **2018**, *25*, 21525–21534. [CrossRef] [PubMed]
6. Xu, G.; Lv, Y.; Sun, J.; Shao, H.; Wei, L. Recent advances in biochar applications in agricultural soils: Benefits and environmental implications. *CLEAN Soil Air Water* **2012**, *40*, 1093–1098. [CrossRef]
7. Diatta, A.A.; Fike, J.H.; Battaglia, M.L.; Galbraith, J.M.; Baig, M.B. Effects of biochar on soil fertility and crop productivity in arid regions: A review. *Arab. J. Geosci.* **2020**, *13*, 1–17. [CrossRef]
8. Murtaza, G.; Ahmed, Z.; Iqbal, R.; Deng, G. Biochar from agricultural waste as a strategic resource for promotion of crop growth and nutrient cycling of soil under drought and salinity stress conditions: A comprehensive review with context of climate change. *J. Plant Nutr.* **2025**, *48*, 1832–1883. [CrossRef]
9. Alkharabsheh, H.M.; Seleiman, M.F.; Battaglia, M.L.; Shami, A.; Jalal, R.S.; Alhammad, B.A.; Almutairi, K.F.; Al–Saif, A.M. Biochar and its broad impacts in soil quality and fertility, nutrient leaching and crop productivity: A review. *Agronomy* **2021**, *11*, 993. [CrossRef]
10. Yin, Y.; Yang, C.; Li, M.; Zheng, Y.; Ge, C.; Gu, J.; Li, H.; Duan, M.; Wang, X.; Chen, R. Research progress and prospects for using biochar to mitigate greenhouse gas emissions during composting: A review. *Sci. Total. Environ.* **2021**, *798*, 149294. [CrossRef] [PubMed]
11. Cao, Y.; Wang, X.; Bai, Z.; Chadwick, D.; Misselbrook, T.; Sommer, S.G.; Qin, W.; Ma, L. Mitigation of ammonia, nitrous oxide and methane emissions during solid waste composting with different additives: A meta-analysis. *J. Clean. Prod.* **2019**, *235*, 626–635. [CrossRef]
12. Xiao, R.; Awasthi, M.K.; Li, R.; Park, J.; Pensky, S.M.; Wang, Q.; Wang, J.J.; Zhang, Z. Recent developments in biochar utilization as an additive in organic solid waste composting: A review. *Bioresour. Technol.* **2017**, *246*, 203–213. [CrossRef]
13. Lyu, H.; Zhang, H.; Chu, M.; Zhang, C.; Tang, J.; Chang, S.X.; Mašek, O.; Ok, Y.S. Biochar affects greenhouse gas emissions in various environments: A critical review. *Land Degrad. Dev.* **2022**, *33*, 3327–3342. [CrossRef]
14. Awasthi, M.K.; Duan, Y.; Awasthi, S.K.; Liu, T.; Zhang, Z. Influence of bamboo biochar on mitigating greenhouse gas emissions and nitrogen loss during poultry manure composting. *Bioresour. Technol.* **2020**, *303*, 122952. [CrossRef]
15. Noor, R.S.; Shah, A.N.; Tahir, M.B.; Umair, M.; Nawaz, M.; Ali, A.; Ercisli, S.; Abdelsalam, N.R.; Ali, H.M.; Yang, S.H.; et al. Recent trends and advances in additive-mediated composting technology for agricultural waste resources: A comprehensive review. *ACS Omega* **2024**, *9*, 8632–8653. [CrossRef]
16. Pires, A.J.; Esteves, C.; Bexiga, R.; Oliveira, M.; Fangueiro, D. Biochar Supplementation of Recycled Manure Solids: Impact on Their Characteristics and Greenhouse Gas Emissions During Storage. *Agronomy* **2025**, *15*, 973. [CrossRef]

17. Stegenta-Dąbrowska, S.; Syguła, E.; Bednik, M.; Rosik, J. Effective carbon dioxide mitigation and improvement of compost nutrients with the use of composts' biochar. *Materials* **2024**, *17*, 563. [CrossRef]
18. Keiluweit, M.; Nico, P.S.; Johnson, M.G.; Kleber, M. Dynamic molecular structure of plant biomass-derived black carbon (biochar). *Environ. Sci. Technol.* **2010**, *44*, 1247–1253. [CrossRef] [PubMed]
19. Lehmann, J.; Joseph, S. Biochar for environmental management: An introduction. In *Biochar for Environmental Management*; Routledge: London, UK, 2015; pp. 1–13.
20. Haug, R.T. *The Practical Handbook of Compost Engineering*; Routledge: Boca Raton, FL, USA, 2018. [CrossRef]
21. Alkoaik, F.; Al-Faraj, A.; Al-Helal, I.; Fulleros, R.; Ibrahim, M.; Abdel-Ghany, A.M. Toward sustainability in rural areas: Composting palm tree residues in rotating bioreactors. *Sustainability* **2019**, *12*, 201. [CrossRef]
22. Heimsch, L. Greenhouse Gas Fluxes and Carbon Balance in Finnish Agroecosystems that Utilise Regenerative Farming Practices. Ph.D. Thesis, University of Helsinki, Helsinki, Finland, 2024.
23. Brummell, M. Greenhouse gas production and consumption in soils of the Canadian High Arctic. Ph.D. Thesis, University of Saskatchewan, Saskatoon, SK, Canada, 2015.
24. US Composting Council. *Test Methods for the Examination of Composting and Compost (TMECC)*; Thompson, W.H., Ed.; U.S. Government Printing Office: Washington, DC, USA, 2002.
25. Chan, M.T.; Selvam, A.; Wong, J.W.C. Reducing nitrogen loss and salinity during 'struvite' food waste composting by zeolite amendment. *Bioresour. Technol.* **2016**, *200*, 838–844. [CrossRef]
26. Berendes, D.; Levy, K.; Knee, J.; Handzel, T.; Hill, V.R. Ascaris and Escherichia coli inactivation in an ecological sanitation system in Port-au-Prince, Haiti. *PLoS ONE* **2015**, *10*, e0125336. [CrossRef]
27. Szabová, E.; Juriš, P.; Papajová, I. Sanitation composting process in different seasons. Ascaris suum as model. *Waste Manag.* **2010**, *30*, 426–432. [CrossRef] [PubMed]
28. Chowdhury, M.A.; de Neergaard, A.; Jensen, L.S. Potential of aeration flow rate and bio-char addition to reduce greenhouse gas and ammonia emissions during manure composting. *Chemosphere* **2014**, *97*, 16–25. [CrossRef]
29. Preneta, N.; Kramer, S.; Magloire, B.; Noel, J.M. Thermophilic co-composting of human wastes in Haiti. *J. Water Sanit. Hyg. Dev.* **2013**, *3*, 649–654. [CrossRef]
30. Chen, H.; Awasthi, S.K.; Liu, T.; Duan, Y.; Ren, X.; Zhang, Z.; Pandey, A.; Awasthi, M.K. Effects of microbial culture and chicken manure biochar on compost maturity and greenhouse gas emissions during chicken manure composting. *J. Hazard. Mater.* **2020**, *389*, 121908. [CrossRef] [PubMed]
31. López-Cano, I.; Roig, A.; Cayuela, M.L.; Alburquerque, J.A.; Sánchez-Monedero, M.A. Biochar improves N cycling during composting of olive mill wastes and sheep manure. *Waste Manag.* **2016**, *49*, 553–559. [CrossRef]
32. Agyarko-Mintah, E.; Cowie, A.; Van Zwieten, L.; Singh, B.P.; Smillie, R.; Harden, S.; Fornasier, F. Biochar lowers ammonia emission and improves nitrogen retention in poultry litter composting. *Waste Manag.* **2017**, *61*, 129–137. [CrossRef]
33. Wang, C.; Lu, H.; Dong, D.; Deng, H.; Strong, P.J.; Wang, H.; Wu, W. Insight into the effects of biochar on manure composting: Evidence supporting the relationship between N_2O emission and denitrifying community. *Environ. Sci. Technol.* **2013**, *47*, 7341–7349. [CrossRef]
34. Kaudal, B.B.; Weatherley, A.J. Agronomic effectiveness of urban biochar aged through co-composting with food waste. *Waste Manag.* **2018**, *77*, 87–97. [CrossRef] [PubMed]
35. Yang, Y.; Awasthi, M.K.; Wu, L.; Yan, Y.; Lv, J. Microbial driving mechanism of biochar and bean dregs on NH_3 and N_2O emissions during composting. *Bioresour. Technol.* **2020**, *315*, 123829. [CrossRef] [PubMed]
36. Castro-Herrera, D.; Prost, K.; Kim, D.; Yimer, F.; Tadesse, M.; Gebrehiwot, M.; Brüggemann, N. Biochar addition reduces non-CO_2 greenhouse gas emissions during composting of human excreta and cattle manure. *J. Environ. Qual.* **2023**, *52*, 814–828. [CrossRef]
37. Chen, W.; Liao, X.; Wu, Y.; Liang, J.B.; Mi, J.; Huang, J.; Zhang, H.; Wu, Y.; Qiao, Z.; Li, X.; et al. Effects of different types of biochar on methane and ammonia mitigation during layer manure composting. *Waste Manag.* **2017**, *61*, 506–515. [CrossRef]
38. Sanchez-Monedero, M.A.; Cayuela, M.L.; Roig, A.; Jindo, K.; Mondini, C.; Bolan, N.J.B.T. Role of biochar as an additive in organic waste composting. *Bioresour. Technol.* **2018**, *247*, 1155–1164. [CrossRef]
39. Waqas, M.; Hashim, S.; Humphries, U.W.; Ahmad, S.; Noor, R.; Shoaib, M.; Naseem, A.; Hlaing, P.T.; Lin, H.A. Composting processes for agricultural waste management: A comprehensive review. *Processes* **2023**, *11*, 731. [CrossRef]
40. Sánchez-García, M.; Alburquerque, J.; Sánchez-Monedero, M.; Roig, A.; Cayuela, M. Biochar accelerates organic matter degradation and enhances N mineralisation during composting of poultry manure without a relevant impact on gas emissions. *Bioresour. Technol.* **2015**, *192*, 272–279. [CrossRef]
41. Liu, W.; Huo, R.; Xu, J.; Liang, S.; Li, J.; Zhao, T.; Wang, S. Effects of biochar on nitrogen transformation and heavy metals in sludge composting. *Bioresour. Technol.* **2017**, *235*, 43–49. [CrossRef]
42. Khan, N.; Bolan, N.; Jospeh, S.; Anh, M.T.L.; Meier, S.; Kookana, R.; Borchard, N.; Sánchez-Monedero, M.A.; Jindo, K.; Solaiman, Z.M.; et al. Complementing compost with biochar for agriculture, soil remediation and climate mitigation. *Adv. Agron.* **2023**, *179*, 1–90.

43. Wang, S.-P.; Wang, L.; Sun, Z.-Y.; Wang, S.-T.; Shen, C.-H.; Tang, Y.-Q.; Kida, K. Biochar addition reduces nitrogen loss and accelerates composting process by affecting the core microbial community during distilled grain waste composting. *Bioresour. Technol.* **2021**, *337*, 125492. [CrossRef]
44. Khan, N.; Clark, I.; Sánchez-Monedero, M.A.; Shea, S.; Meier, S.; Qi, F.; Kookana, R.S.; Bolan, N. Physical and chemical properties of biochars co-composted with biowastes and incubated with a chicken litter compost. *Chemosphere* **2016**, *142*, 14–23. [CrossRef] [PubMed]
45. Forján, R.; Rodríguez-Vila, A.; Cerqueira, B.; Covelo, E.F.; Marcet, P.; Asensio, V. Comparative effect of compost and technosol enhanced with biochar on the fertility of a degraded soil. *Environ. Monit. Assess.* **2018**, *190*, 610. [CrossRef] [PubMed]
46. Novak, J.M.; Ippolito, J.A.; Watts, D.W.; Sigua, G.C.; Ducey, T.F.; Johnson, M.G. Biochar compost blends facilitate switchgrass growth in mine soils by reducing Cd and Zn bioavailability. *Biochar* **2019**, *1*, 97–114. [CrossRef]
47. Ye, S.; Zeng, G.; Wu, H.; Liang, J.; Zhang, C.; Dai, J.; Xiong, W.; Song, B.; Wu, S.; Yu, J. The effects of activated biochar addition on remediation efficiency of co-composting with contaminated wetland soil. *Resour. Conserv. Recycl.* **2019**, *140*, 278–285. [CrossRef]